Physical and electrochemical properties of LiFePO$_4$/carbon composite synthesized at various pyrolysis periods

Kuei-Feng Hsu [a], Sun-Yuan Tsay [a], Bing-Joe Hwang [b],*

[a] *Department of Chemical Engineering, National Cheng Kung University, No. 1, Ta-Hsueh Road, Tainan 701, Taiwan, ROC*
[b] *Department of Chemical Engineering, National Taiwan University of Science and Technology, 43 Keelung Road, Sec. 4, Taipei 106, Taiwan, ROC*

Abstract

Aluminum-doped lithium iron phosphate was synthesized with a modified sol–gel process. The sol–gel derived cathodes show much higher conductivity than those prepared by a solid-state method. The conductivity is 8×10^{-2} S cm^{-1} for the Al-doped LiFePO$_4$/carbon composite powders synthesized at 850 °C for 2 h, as determined using AC impedance spectroscopy. The electrodes consisting of the Al-doped LiFePO$_4$/carbon composite powders were fabricated for the electrochemical characterization and showed a specific capacity of about 150 mAh g^{-1} at C/40 rate. Not only the conductivity of the crystal lattice but also the conductivity of the grain boundary is enhanced for the nano-sized Al-doped LiFePO$_4$/carbon composite powders.
© 2005 Elsevier B.V. All rights reserved.

Keywords: Nano-composite; LiFePO$_4$; Cathode material; Conductivity

1. Introduction

The crystal structure of LiFePO$_4$, which has been studied by O.V. Yakubovich, M.A. Simonov, and N.V. Belov (1977) and described in more detail by O.V. Yakubovich, E.L. Belkoneva, V.G. Tsirelson, and V.S. Urusov (1990), has an olivine-type structure with a distorted hexagonal anion close packing, where the cations occupy three different positions: a tetrahedral (P) site and two octahedral sites. One octahedral site lies at the inversion centre and the other is in the mirror plane. As usual in olivine-type structures, the former octahedral site is occupied by cations with smaller charge (Li) and the latter by cations with larger charge (Fe). The main feature of the LiFePO$_4$ crystal structure consists of olivine-type ribbons extending along the *b* crystal axis. The Li octahedral protrude from the olivine ribbon and are connected along their edges and with the larger Fe octahedral. PO$_4$ tetrahedral have three of the six edges in common with the cation octahedral. These edges have the shortest lengths and differ significantly from the other O–O distances [1].

Lithium ion phosphate is considered a promising cathode material for lithium batteries due to its low cost, high capacity, a toxic and high energy density. It was reported that olivine LiFePO$_4$ discharged at 3.4 V versus Li/Li$^+$ and cycled well at ambient temperature with a reversible capacity of 120 mAh g^{-1} by Padhi et al. [2]. Subsequently, extensive work on LiFePO$_4$ has been carried out by a number of groups [3–6]. However, the main problem with this material is low electric conductivity and therefore many researchers are working on developing strategies to improve its conductivity, such as metal dispersion, carbon coating, co-synthesizing with carbon, etc. [7–10]. These improvements could not increase the lattice electronic conductivity within the crystal, and according to the first principle calculations revealed LiFePO$_4$ is a semiconductor with ca. 0.3 eV band gap. So, if cation-deficient solid solutions could be retained, good p-type conductivity should result. On the other hand, substitution of Li$^+$ or Fe^{2+} with supervalent cations might be expected to result in increased n-type conductivity. In 2002, Chung et al. [11] reported that the electronic conductivity of LiFePO$_4$ was enhanced by a factor $\sim 10^8$ (10^{-2} S cm^{-1}) by controlling the cation non-stoichiometry combined with solid-solution doping of supervalent cations. These

materials doped with about 1% metal ions have capacity of about 140 mAh g^{-1} at C/10 rate. Al-doped LiFePO$_4$/carbon composite powders were synthesized with a modified sol–gel process in which formation of conductive carbons and metal doping were achieved simultaneously. The conductivity and electrochemical properties of the synthesized composite powders are discussed in this work.

2. Experimental

Li$_{0.99}$Al$_{0.01}$FePO$_4$ samples were synthesized by a sol–gel method using citric acid as a chelating agent [12]. Stoichiometric amounts of iron powder, aluminum nitrate nonahydrate, and lithium nitrate were dissolved in 200 ml of a solution of citric acid with continuous stirring. To this solution, 10 ml of a saturated aqueous solution of ammonium dihydrogen phosphate was then added. In these experiments, the molar ratio of chelating agent to the total metal ion was maintained at unity. The mixtures were heated gently with continuous stirring for 4 h to remove excess water. The resulting gel precursor was dried in a circulation oven for a week at 60 °C. The precursors were further calcined at 850 °C in 99.99% nitrogen atmosphere for 2, 10, 20, and 30 h. The heating rate of the furnace was 10 °C min^{-1}.

To determine the carbon content, elemental analysis was performed (EA; Heraeus CHN-O Rapid Analyzer). Phase purity was verified from the powder X-ray diffraction (XRD; Rigaku, RINT2000) using Cu Kα radiation with 2θ in the range from 10° to 60° at a scan rate of 1° min^{-1}. The conductivity of the Li$_{0.99}$Al$_{0.01}$FePO$_4$ was measured on the pressed pellet using the Autolab PGSTAT 30 equipment (Euo Chemie B.V., The Netherlands) with the frequency response analysis (FRA) software under an oscillation potential of 10 mV from 0.95 MHz to 0.01 Hz. The surface morphology of the powders after calcination was observed with a field emission scanning electron microscopy (FE-SEM; JEOL, 6500F). The nano-scale microstructure was examined using a transmission electron microscopy (TEM; JEOL, JEM 1010). The samples were dispersed into water and the suspension solution was dropped on a standard copper TEM grid. The disordering of graphite was examined by Raman spectroscopy in the range of 1200–1850 cm^{-1} (dilor XY with Ar ion laser of 20 mW at 514 nm). Electrochemical characterization was carried out with coin-type cells. The electrode was prepared by using 83% of LiFePO$_4$/carbon active material, 11% Super P carbon black and 6% polyvinylidene difluoride (PVdF), as binder, dissolved in n-methyl pyrrolidinone (NMP) solvent. The obtained slurry was then cast on the Al current collector and dried for 2 h in an oven at 100 °C. The resulting electrode film was subsequently pressed and punched into a circular disc. The electrode films are preserved in an argon-filled glove box (Unilab, Mbruan). The coin cell was fabricated using the lithium metal as a counter electrode. The electrolyte used consisted of a 1 M solution of LiPF$_6$ in a mixture 1:1 by volume of ethylene carbonate (EC) and diethyl carbonate (DEC).

The separator (Celgard 2400, Hoechst Celenese Corp.) was soaked in an electrolyte for 24 h prior to use. All the weighing procedure and coin cell assembly were performed in the argon-filled glove box by keeping both oxygen and moisture level less than 1 ppm. The charge–discharge measurements were performed on the coin cell using the programmable battery tester (Maccor 2300) at different C-rates over a potential range of 3.0–4.0 V.

3. Results and discussion

3.1. XRD analysis

Fig. 1 shows the XRD profiles of Li$_{0.99}$Al$_{0.01}$FePO$_4$ synthesized at 850 °C for 2, 10, 20, and 30 h. All samples were single-phase Li$_{0.99}$Al$_{0.01}$FePO$_4$ with an ordered olivine structure indexed by orthorhombic Pnmb (JCPDS card no. 40-1499). There is no evidence for the formation of crystalline or amorphous carbons. This is undoubtedly because the presence of the formed carbon is too small or the thickness of the formed carbon on the nano-sized Li$_{0.99}$Al$_{0.01}$FePO$_4$ powders is too thin. As the sintering time is increased from 2 to 30 h, the amount of carbon in the composite powders decreased from 10% to 0.2%, as determined using element analysis (EA). Meanwhile, the conductivity of the composite powders decreases from 10^{-2} to 10^{-7} S cm^{-1}, as determined using AC impedance. The grain size (t) was calculated using the Scherrer's equation: $\beta \cos(\theta) = 0.9\lambda/t$, where β is the full-width-at-half-maximum length of the diffraction peak on a 2θ scale. From the Scherrer's equation D$_{131}$ values for the sintering time 2, 10, 20, and 30 h are 47, 48, 50, and 51 nm, respectively. The grain size of the Al-doped LiFePO$_4$ is similar to that of the undoped LiFePO$_4$ at the same sintering condition. The grain size of the Al-doped LiFePO$_4$ is increased insignificantly with sintering time in the developed process. It is obviously observed that the growth of the LiFePO$_4$ grains is inhibited by the formed carbons. The phenomenon is consistent with our previous report [12], in-
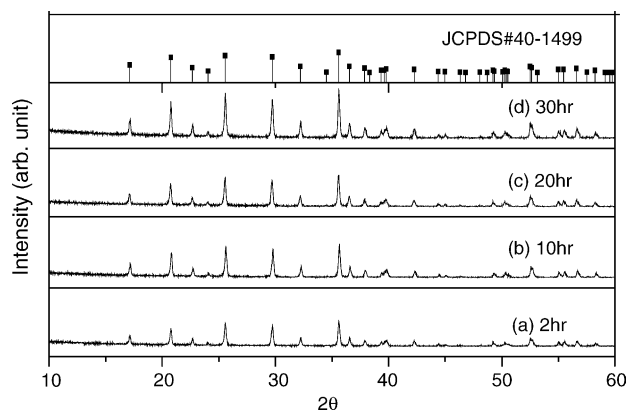

Fig. 1. X-ray diffraction patterns using Cu Kα radition for Li$_{0.99}$Al$_{0.01}$FePO$_4$ sintered at 850 °C for 2, 10, 20, and 30 h, respectively.
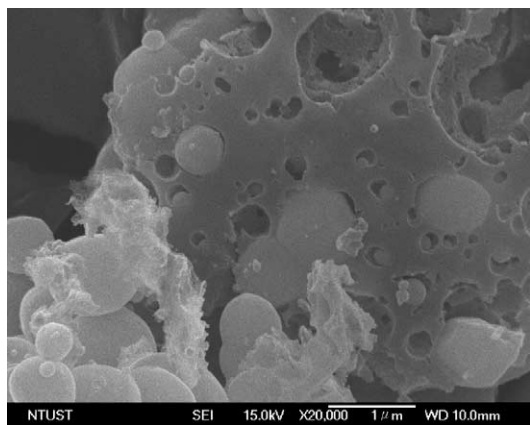
Fig. 2. A FE-SEM micrograph of a nano-composite $Li_{0.99}Al_{0.01}FePO_4$/carbon sintered at 850 °C for 2 h.

dicating that the nano-sized $LiFePO_4$ and its derivatives can be obtained by the developed sol–gel process.

3.2. Morphology

Micro-sized $Li_{0.99}Al_{0.01}FePO_4$ powders were found inside the pores of the carbon network formed during the sintering process, as shown in Fig. 2. The formed carbon network shows circle-type micropores with narrow pore size distribution. The pore size of the formed carbon network is around 1 μm observed from the SEM image. The particle size of the synthesized $Li_{0.99}Al_{0.01}FePO_4$ powder is larger than its grain size, implying that the particles are formed from the agglomeration of several grains. Meanwhile, the particle growth is limited in the micropores of the carbon network, resulting in the formation of the micro-sized $Li_{0.99}Al_{0.01}FePO_4$ particles. From the TEM image, it can be seen that the micro-sized $Li_{0.99}Al_{0.01}FePO_4$ particle consists of several nano-sized $Li_{0.99}Al_{0.01}FePO_4$ grains coated with the formed carbon. Fig. 3 shows the TEM bright field images of the formed carbon network. In this image, the dark ~50 nm spots represent the $Li_{0.99}Al_{0.01}FePO_4$ grains. The size of the $Li_{0.99}Al_{0.01}FePO_4$ grain is in good agreement with the D_{131} crystalline size obtained from the X-ray diffraction pattern. The grain size of $Li_{0.99}Al_{0.01}FePO_4$ particles in the range of 47–51 nm is obtained at sintering time from 2 to 30 h. The grain growth is insignificant during sintering, implying that the grain growth is impeded by the thin layer of the formed carbon on the surface of the grain. It is worthy to note that the conductivity of the particles can be enhanced because of the existence of the formed carbon between the grains in the particles. A scheme of the nano-sized $Li_{0.99}Al_{0.01}FePO_4$/carbon composite particles is proposed based on the TEM observation, as shown in Fig. 4.

3.3. Raman spectra

Fig. 5 displays the Raman spectra of the $Li_{0.99}Al_{0.01}FePO_4$ powders synthesized at 850 °C for various periods in the

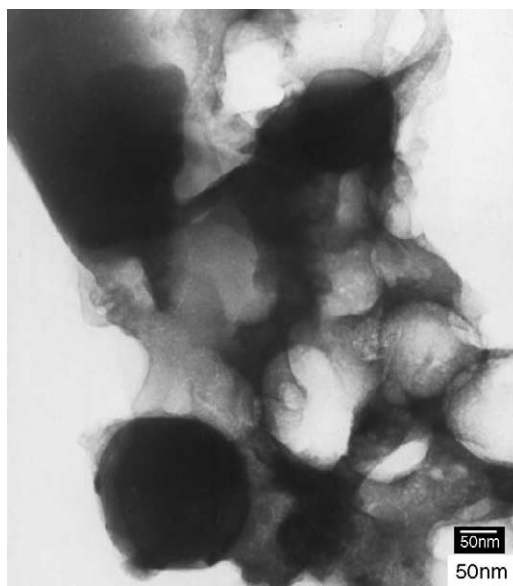Fig. 3. A TEM micrograph of a nano-composite $Li_{0.99}Al_{0.01}FePO_4$/carbon sintered at 850 °C for 2 h.

range of 1200–1850 cm^{-1}. The broad bands at 1354 and 1591 cm^{-1} are well known from the spectroscopy of carbon as being the D band and G band that originate from amorphous and graphitic forms, respectively. The peak intensity ratios in Raman shifts between 1354 and 1591 cm^{-1} calculated as R-values (I_D/I_G) can be employed to evaluate the degree of disordering. These results indicate that the citric acid can be pyrolyzed to form highly graphitized carbons with low I_D/I_G ratios and good electronic properties
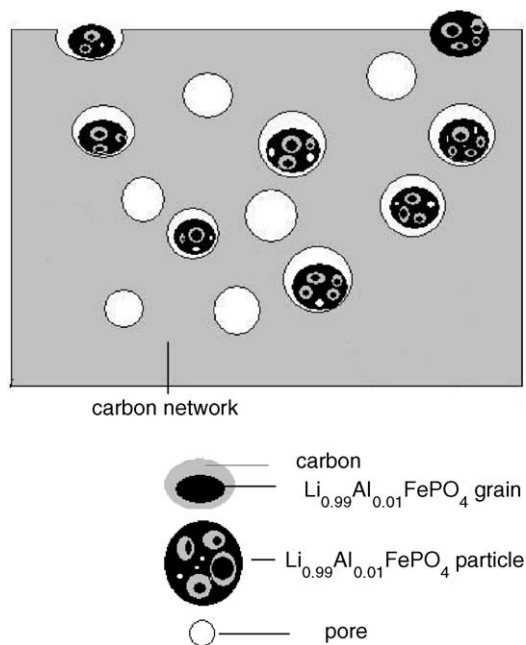

Fig. 4. Schematic model of the nano-sized $Li_{0.99}Al_{0.01}FePO_4$/carbon composite particle.

[13]. As the sintering time is increased from 2 to 30 h, the I_D/I_G ratio of $Li_{0.99}Al_{0.01}FePO_4$/carbon increases from 0.98 to 1.24, suggesting the conductivity of the formed carbon increases with the sintering time. However, the conductivity of the composite powders decreases with an increase in the sintering time at 850 °C, indicating that decreasing the amount of carbon leads to decrease their conductivity. The percolation of the carbon network is extremely critical for the conductivity of the composite $Li_{0.99}Al_{0.01}FePO_4$/carbon powders. The conductivity of the composite powders decreases dramatically if the carbon content is less than a percolation value.

3.4. Electrochemical properties

The cycling behavior of the material is strongly dependent on temperature [14] and carbon content [12,15]. The electrochemical properties of the $Li_{0.99}Al_{0.01}FePO_4$ sample synthesized at 850 °C for various sintering times (2, 10, 20, and 30 h) were evaluated. The carbon content in the synthesized composite powders is 10, 3, 0.3, and 0.2 wt.% at sintering time of 2, 10, 20, and 30 h, respectively. There is no electrochemical activity observed for the samples synthesized at the sintering time of 10, 20, and 30 h although the $Li_{0.99}Al_{0.01}FePO_4$ powders with good crystallinity and without-impurity phase were obtained. It indicates that the carbon content in the composite powders is not enough to provide a network for electronic conduction. Consequently, the electrochemical activity for those samples could not be obtained at 1/40 C. The material synthesized at 850 °C for 2 h showed the best cell performance, as is shown in Fig. 6. The reversible capacity obtained for the material synthesized at 850 °C for 2 h is 150 mAh g^{-1}. Fig. 5 shows the voltage profile for the cell cycled at 1/40 C in the po-
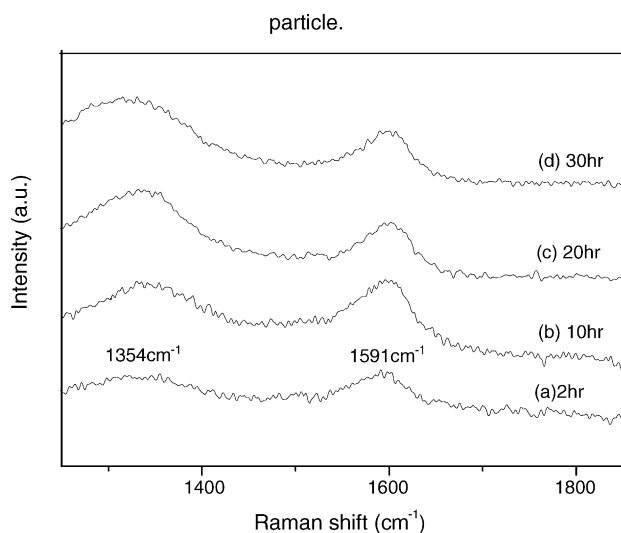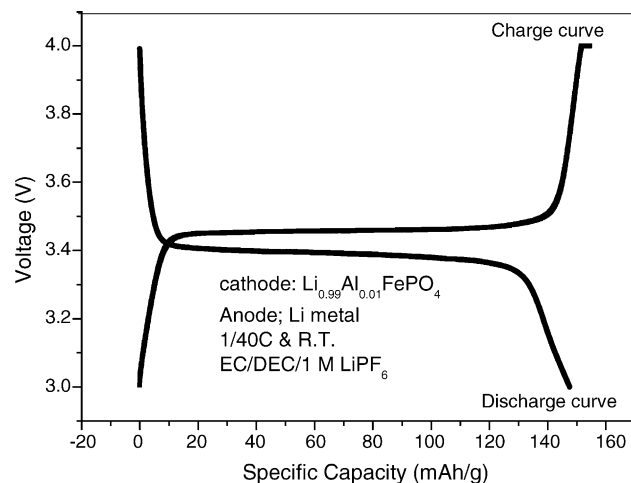

Fig. 6. Initial voltage profiles of $Li_{0.99}Al_{0.01}FePO_4$/carbon sintered at 850 °C for 2 h (1/40 C).

tential range of 3.0–4.0 V at room temperature. The cell voltage quickly increases from the end charge potential (3.0 V) to about 3.46 V and then it grows with an exponential fashion. During the galvanostatic charge, the cathode was able to accommodate about 98% of the total capacity while a further 2% was accommodated during the constant voltage charge. During the discharge the voltage drops quickly down to 3.39 V; after which it is almost independent of the degree of reduction. A two-phase reaction takes place at this plateau. It is consistent with the report in the literature. When the cell is discharged to about 91% of the capacity, the voltage drops below 3.0 V and then falls sharply.

4. Conclusions

The $Li_{0.99}Al_{0.01}FePO_4$/carbon composite powders composed of conductive carbon and micro-sized $Li_{0.99}Al_{0.01}FePO_4$ particles were synthesized by the developed sol–gel process. The micro-sized composite particles consist of nano-sized $Li_{0.99}Al_{0.01}FePO_4$ grains coated with the formed carbon. A scheme was proposed for the micro-sized composite powders. The enhancement of the conductivity of the composite powders can be contributed from formation of the micro-sized composite powders. Increasing the sintering time leads to decrease in the conductivity of the $Li_{0.99}Al_{0.01}FePO_4$/carbon composite powders because the carbon content is too low to from a conductive network while the sintering time is higher than 3 h. The electronic conductivity of the $Li_{0.99}Al_{0.01}FePO_4$/carbon composites is greatly improved, reaching a value of 8×10^{-2} S cm^{-1} at room temperature. It was found that the electrochemical properties of the synthesized $Li_{0.99}Al_{0.01}FePO_4$/carbon composite are improved because of its small grain size and good electronic conductivity.

Fig. 5. Raman spectra of $Li_{0.99}Al_{0.01}FePO_4$/carbon powders at different sintering time by the sol–gel method. From bottom to top 2, 10, 20, and 30 h, respectively.

Acknowledgements

References

[1] V.A. Streltsov, E.L. Belokoneva, V.G. Tsirelson, N. Hansen, Multipole analysis of the electron density in triphylite $LiFePO_4$ using X-ray diffraction data, Acta Crystallogr. B49 (1993) 147.

[2] A.K. Padhi, K.S. Nanjundaswamy, J.B. Goodenough, J. Electrochem. Soc. 144 (1997) 1188.

[3] N. Ravet, Y. Chouinard, J.F. Magnan, S. Besner, M. Gauthier, M. Armand, J. Power Sources 97 (2001) 503.

[4] F. Croce, A.D. Epifanio, J. Hassoun, A. Deptula, T. Olczac, Electrochem. Solid State Lett. 5 (2002) A47.

[5] M. Takahashi, S.-i. Tobishima, K. Takei, Y. Sakurai, Solid State Ionics 148 (2002) 283.

[6] P.P. Prosini, M. Carewska, S. Scaccia, P. Wisniewski, M. Pasquali, Electrochim. Acta 48 (2003) 4205.

[7] S.-Y. Chung, J.T. Bloking, Y.-M. Chiang, Nat. Mater. 1 (2002) 123.

[8] S. Yang, P.Y. Zavalij, M.S. Whittingham, Electrochem. Commun. 3 (2001) 505.

[9] N. Ravet, Y. Chouinard, J.F. Magnan, S. Besner, M. Gauthier, M. Armand, J. Power Sources 97 (2001) 503.

[10] H. Huang, S.-C. Yin, L.F. Nazar, Electrochem. Solid State Lett. 4 (2001) A170.

[11] S.-Y. Chung, J.T. Bloking, Y.-M. Chiang, Nat. Mater. 1 (2002) 123.

[12] K.-F Hsu, S.-Y Tsay, B.J. Hwang, J. Mater. Chem. (2004), DOI: 10.1039/b406774f.

[13] M.M. Doeff, Y. Hu, F. McLarnon, R. Kostecki, Electrochem. Solid State Lett. 6 (2003) A207.

[14] A.S. Andersson, J.O. Thomas, B. Kalska, L. Haggstrom, Electrochem. Solid State Lett. 3 (2000) 66.

[15] Z. Chen, J.R. Dahn, J. Electrochem. Soc. 149 (2002) A1184.